Biochemical and Biophysical Research Communications 429 (2012) 12–17

Contents lists available at SciVerse ScienceDirect

Biochemical and Biophysical Research Communications

journal homepage: www.elsevier.com/locate/ybbrc

ANT-VDAC1 interaction is direct and depends on ANT isoform conformation *in vitro*

Maya Allouche [a], Claire Pertuiset [b,c], Jean-Luc Robert [d], Cécile Martel [b,c], Rémi Veneziano [a], Céline Henry [e], Ossama Sharaf el dein [b,c], Nathalie Saint [f], Catherine Brenner [b,c,*], Joel Chopineau [a,d,*]

[a] *UMR 5253 CNRS-ENSCM UM2-UM1, Montpellier, France*
[b] *INSERM UMR-S 769, LabEx LERMIT, Châtenay-Malabry, France*
[c] *Université Paris-Sud, Châtenay-Malabry, France*
[d] *Université de Nîmes, Nîmes, France*
[e] *Plateforme Protéomique, Unité Micalis, INRA Jouy-en-Josas, France*
[f] *INSERM U1046, Montpellier, France*

ARTICLE INFO

Article history:
Received 12 October 2012
Available online 3 November 2012

Keywords:
Channel
Liposome
Mitochondrion
Surface plasmon resonance

ABSTRACT

The voltage-dependent anion channel (VDAC) and the adenine nucleotide translocase (ANT) have central roles in mitochondrial functions such as nucleotides transport and cell death. The interaction between VDAC, an outer mitochondrial membrane protein and ANT, an inner membrane protein, was studied in isolated mitochondria and *in vitro*. Both proteins were isolated from various mitochondrial sources and reconstituted *in vitro* using a biomimetic system composed of recombinant human VDAC isoform 1 (rhVDAC1) immobilized on a surface plasmon resonance (SPR) sensor chip surface. Two enriched-preparations of $_{H}$ANT (ANT from heart, mainly ANT1) and $_{L}$ANT (ANT from liver, mainly ANT2) isoforms interacted differently with rhVDAC1. Moreover, the pharmacological ANT inhibitors atractyloside and bongkrekic acid modulated this interaction. Thus, ANT-VDAC interaction depends both on ANT isoform identity and on the conformation of ANT.

1. Introduction

Mitochondria play multiple roles in cellular pathophysiology such as energy and lipid metabolism, reactive oxygen species production and detoxification and cell death [1]. These organelles are delimitated by two membranes that differ largely by their composition, surface and function. The outer membrane (OM) constitutes a permeable barrier that allows metabolites, ions and water fluxes trough dedicated channels such as the voltage-dependent anion channel or porin (VDAC) [2]. VDAC is the most abundant OM integral protein. It is expressed as three isoforms in mammals, VDAC1 to 3, which span the OM with 19 β strands [3]. VDAC channel can be modulated by calcium (Ca^{2+}), anion superoxide, phosphorylation and interaction with cytosolic proteins, all of which influencing cell metabolism and cell fate [4]. In contrast, the inner membrane (IM) delimitates the boundary between the intermembrane space and the matrix. The exchange of metabolites and ions on IM is mainly mediated by mitochondrial carriers [5]. One of them is the adenine nucleotide translocase (ANT) [6], which is encoded by three or four tissue-specific isoforms in mammals, namely ANT1 to ANT4. In normal conditions, ANT is a stoichiometric ADP/ATP translocase, but in the presence of various ligands *in vitro* (e.g. Ca^{2+}), ANT can behave as a channel, whose conductance can be enhanced by interaction with Bax [7–9]. The bovine ANT1 has been co-crystallized with carboxyatractyloside confirming *in silico* prediction of six transmembrane helices with *N* and *C* terminus facing the intermembrane space [10]. However, despite a lack of consensus on the monomeric *versus* dimeric status of ANT, it can be found in hetero-oligomers, such as the permeability transition pore (PTP) [8,11,12] and the ATP synthasome [13]. These associations would depend on tissue and pathophysiological conditions [14].

Previously, an ANT-VDAC interaction has been evidenced by co-immunoprecipitation and co-localization approaches [11,15]. This interaction might occur at definite contact sites between OM and IM to facilitate metabolites channeling and/or, upon stimulation, to trigger a sudden phenomenon named permeability transition (PT) [16]. How ANT and VDAC interact is crucial either for the understanding of basic molecular mechanisms of mitochondrial (dys) function or for drug design, but to our knowledge, the interaction is poorly characterized. Therefore, we demonstrated for the first time the direct interaction between ANT and VDAC *in vitro* and unraveled some aspects of its regulation in isolated mitochondria and in a biomimetic system by SPR.

* Corresponding authors. Addresses: INSERM UMR-S 769, LabEx LERMIT, Châtenay-Malabry, France (C. Brenner), UMR 5253 CNRS-ENSCM UM2-UM1, Montpellier, France (J. Chopineau).
E-mail addresses: catherine.brenner-jan@u-psud.fr (C. Brenner), joel.chopineau@unimes.fr (J. Chopineau).

0006-291X/$ - see front matter © 2012 Elsevier Inc. All rights reserved.
http://dx.doi.org/10.1016/j.bbrc.2012.10.108

2. Material and methods

2.1. Isolation of mitochondria and functional assays

Mitochondria were isolated from freshly excised rat heart or liver according to [17,18]. Mitochondrial swelling was assessed by the decrease the mitochondrial suspension (25 μg proteins) in optical density at 540 nm and depolarization was monitored by using an 1 μM rhodamine 123 fluorescence dequenching assay (λ_{exc}: 485 nm, λ_{em}: 535 nm) as previously described [17].

2.2. Immunoprecipitation

ANT was immunocaptured from rat heart mitochondrial extracts by using monoclonal antibody against ANT1 cross-linked to agarose beads (MitoSciences, Eugene, Oregon, US). The immune complexes were separated by SDS-PAGE and electro-transferred for western-blot detection by chemiluminescence, using antibodies against ANT (MitoSciences) and VDAC (Genosphere, Paris, France).

2.3. Production of proteins

A recombinant human C-terminated histidine-tagged VDAC isoform 1 (rhVDAC1) was produced into *E. coli* XL-1 Blue strain (Agilent, US) according to [19]. Briefly, the biomass was suspended in buffer A (1:50 v/v, 20 mM Tris, pH 7.9, 200 mM NaCl and 1 mM PMSF). Inclusion bodies were solubilized in buffer B (1:20 v/v, 6 M urea–HCl, 20 mM Tris–HCl, pH 7.9, 500 mM NaCl, and 10% glycerol) at 4 °C for 30 min. The denatured protein was purified using a Ni-NTA (nitrilotriacetic acid) resin (Qiagen, Germany). It was refolded at 4 °C into refolding buffer (25 mM sodium phosphate pH 7.0, 100 mM NaCl, 1 mM EDTA, 5 mM DTT, 2% lauryl dimethylamine oxide (LDAO)).[20] Single channel activity of VDAC was measured in azolectin planar lipid bilayers. Chambers defined as *cis* and *trans* contained 1 M KCl, 10 mM HEPES, pH 7.4 with 0.5 mM $CaCl_2$, where *cis* was virtually grounded. Proteins were added to the *cis* chamber and the amplified current signals (amplifier BLM 120, Bio-logic) were filtered and analyzed as previously described [21].

2.4. ANT purification and ADP/ATP exchange measurement

Heart ANT was purified to homogeneity from rat hearts according to [8,22] and from liver in the presence of protease inhibitors cocktail from Roche (Bale, Switzerland) and phenylmethanesulfonylfluoride (PMSF). Protein concentration was determined by BCA assay and ANT containing fractions were checked for purity using silver staining and western-blot for ANT, VDAC and Cyclophilin D (Mitosciences). ANT was reconstituted into phosphatidylcholine/cardiolipin (1:45 w:w) liposomes (300 ng ANT per mg lipid) and its function was measured as described [15].

2.5. Protein interaction measurements using SPR

SPR measurements were performed on a Biacore 2000 instrument using Nitrilotriacetate (NTA) sensors chips. rhVDAC1 in interaction buffer (10 mM HEPES, pH 7.4, 150 mM NaCl, 0.005% surfactant P20) was injected at a flow rate of 20 μL min^{-1}. rhVDAC1 coverage was between 850 and 1600 RU corresponding to 85–160 ng/cm^2 (2.5–4.6 pmol/cm^2). Regeneration of the Ni NTA surface could be obtained after injection of running buffer containing 350 mM EDTA at pH 8.3. For interactions, proteins were injected for 300 s at a flow rate of 20 μL min^{-1}. The amount of protein bound to the surface was measured 200 s after reversion to running buffer.

2.6. Mass spectrometry analysis

The identity of ANT and VDAC was confirmed by nano liquid chromatography (LC) coupled to tandem mass spectrometry (MS) as described [23].

3. Results

It is well known that isolated mitochondria treated by Ca^{2+} undergo permeability transition (PT) [24]. Mitochondria were isolated from rat liver and heart by standard procedures and treated by agents to modify the conformation of ANT and determine the impact of these molecules on membrane permeability. Thus, atractyloside (Atra) that inhibits ANT ADP/ATP translocase activity at low doses can also induce PT when used at higher doses (Fig. 1). In contrast, bongkrekic acid (BA), inhibits the translocase function [25,26], but does not induce PT (Fig. 1). Here, we found that Atra induced a dose-dependent decrease in the absorbance of the mitochondrial suspension and in the inner transmembrane potential, $\Delta\Psi m$ (Fig. 1A, B). BA, whose chemical structure is not related to Atra (Fig 1C, D) but binds also to ANT, fully inhibited Atra-induced swelling and depolarization (Fig. 1A, B). This indicates that a change in ANT conformation can affect membrane permeability and ANT interaction with partners.

Irrespective of isoform identity, VDAC has been described to co-immunoprecipitate with ANT in many tissues or cells such as rat liver and human cancer cell lines. Here, we observed that using a specific anti-ANT1 mAb, ANT could be co-immunoprecipitated with VDAC from heart mitochondria in the presence of the surfactant lauryldimethylamine-oxide (LDAO) (Fig. 1E). Interestingly, ANT1 and 2 isoforms were found in the immune complex together with VDAC1, 2 and 3 when analyzed by liquid chromatography and mass spectrometry (Table 1). When mitochondria were pre-treated with Atra and BA, both compounds affected the conformation of ANT since they interrupted the interaction of the ANT-VDAC complex (not shown).

Since immunoprecipitation failed to demonstrate whether some specificity exist in the interactions of various isoforms, we decided to explore the possibility of a direct interaction between ANT and VDAC *in vitro*, using a recombinant human C-terminated histidine-tagged VDAC isoform 1 [19]. The protein was recovered as a highly purified fraction of about 0.5 mg/ml (15 μM) as shown on SDS-PAGE (Fig. 2A). The secondary structure of the rhVDAC1 was appreciated from circular dichroism (CD) (Fig. 2B). The CD spectra recorded in the far ultraviolet for rhVDAC1 in LDAO micelles shows the basic features of beta-barrel porins, which are large positive ellipticity below 205 nm and a broad, less intense minimum centered near 215 nm. The channel activity of rhVDAC1 was checked by channel conductance measurements (Fig. 2C). At low membrane potentials, typically below 30 mV (see recordings at ±10 mV), a permanently open state of channels was measured, whilst at higher voltages (see recordings at ±40 mV) closing events and numerous sub conductance states were observed.

Next, we investigated the interactions of rhVDAC1 with two isoforms ANT1 and ANT2 that were obtained from rat heart and liver, respectively; according to the known ANT isoform organ repartition [27–29]. $_H$ANT (ANT from heart, mainly ANT1) was purified from rat heart mitochondria and $_L$ANT (ANT from liver, mainly ANT2) from rat liver. Analysis by liquid chromatography and mass spectrometry confirmed the presence of ANT1 and 2, but neither ANT3 nor ANT4 in the fractions (not shown). ANTs were purified to homogeneity in concentration of about 0.1 mg/mL (3 μM). The

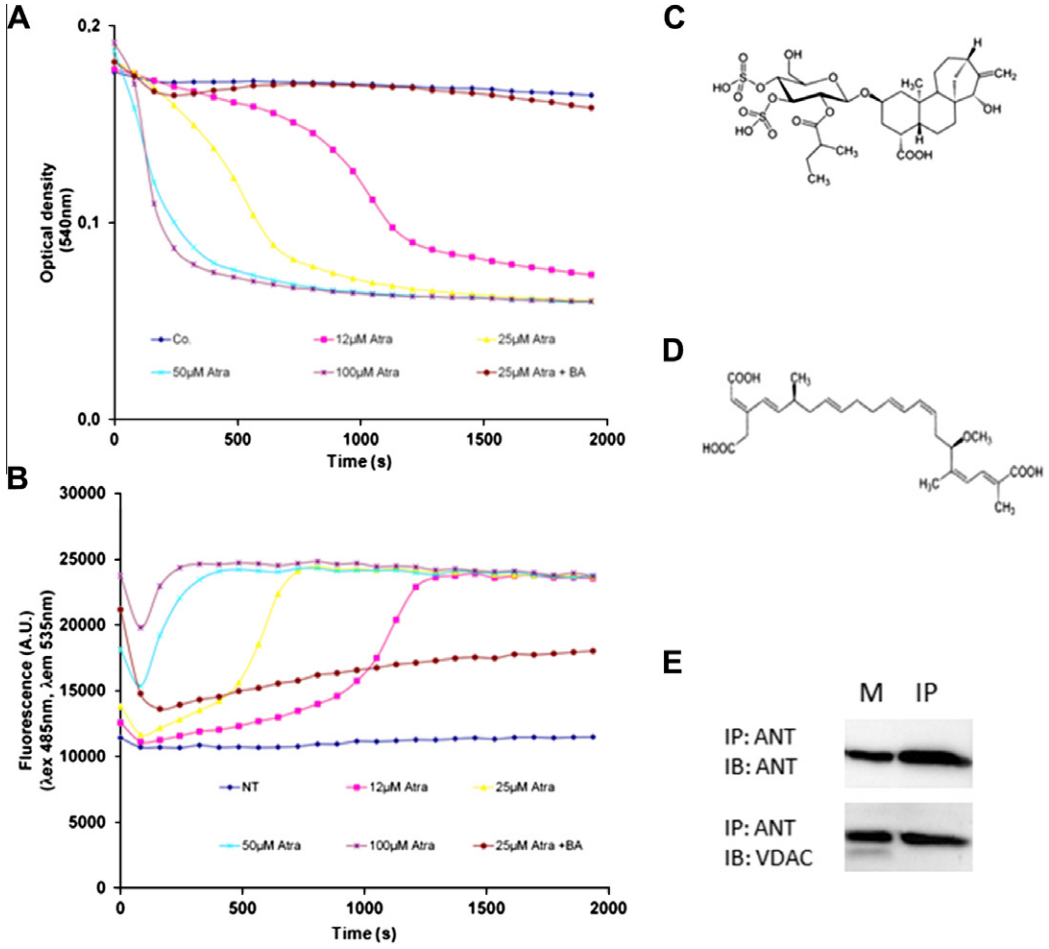

Fig. 1. ANT-VDAC interaction in mitochondria. (A) For swelling experiments, the mitochondrial suspension has been treated by various doses of atractyloside (Atra), bongkrekic acid (BA) or not (Co.) and the optical density (at 540 nm) has been measured for 30 min. (B) Mitochondria pre-loaded with the 1 μM Rhodamine 123, have been treated as in (A) and fluorescence changes reflecting the transmembrane potential measurement have been measured simultaneously for 30 min. The values are means of triplicate samples and the error bars indicate standard deviations. (C) Chemical formula of Atra. (D) Chemical formula of BA. (E) ANT has been co-immunoprecipitated with VDAC from mitochondrial extracts. The immune complexes have been separated by SDS-PAGE and immunoblotted for ANT or VDAC. The experiment has been reproduced three times and yielded to similar results.

Table 1
Identification of ANT and VDAC isoforms. Proteins were co-immunoprecipitated from rat heart mitochondrial extracts in the presence of LDAO using an anti-ANT1 monoclonal antibody. Proteins were separated by SDS-PAGE and submitted to mass spectrometry analysis.

Protein (acc. number)	MW (kDa)	Sequence coverage (%)	Number of peptides
ANT1 (Q05962)	32.9	72	41
ANT2 (Q09073)	32.8	67	36
VDAC1 (Q9Z2L0)	30.8	76	19
VDAC2 (P81155)	31.6	58	12
VDAC3 (Q9R1Z0)	30.7	64	23

purity of ANT preparations was checked by SDS-PAGE with silver staining (not shown) and the absence of detectable contaminating proteins, such as VDAC and cyclophilin D (CypD) was examined by western blotting (Fig. 2D). To check the functionality of purified $_{H}$ and $_{L}$ANT, their capacity to exchange ADP and ATP was measured into proteoliposomes (Fig. 2E). As expected from literature [6,22] both mitochondrial carriers exchanged ADP for ATP and failed to exchange AMP. Of note, $_{H}$ and $_{L}$ANT were inhibited by BA.

The interaction of $_{H}$ANT and $_{L}$ANT with immobilized rhVDAC1 was then evaluated by SPR. The presence of an Histag at the C terminus of the protein allowed for an oriented immobilization of rhVDAC1 on top of an Ni NTA surface. rhVDAC1 was injected in running buffer at concentrations ranging from 0.2 to 450 μM. A maximum coverage of about 4000 RU corresponding to a surface coverage of 4 ng/mm^2 of protein was obtained (data not shown). A surface coverage of 1000–1800 RU (1–2 ng/mm^2) was obtained for injections of rhVDAC1 solution of 0.4 μM and was used for subsequent experiments. As controls, heat denatured $_{H}$ANT and $_{L}$ANT bind neither to the rhVDAC1-coated chip nor to the free rhVDAC1 NiNTA surface. Ionic strength (mainly due to NaCl in our experimental set-up) and surfactants are known to influence drastically protein-protein interactions. Accordingly, the interaction of $_{H}$ANT and $_{L}$ANT with immobilized rhVDAC1 was lowered when NaCl concentration increased (Fig. 3A). Moreover, a lower (4- to 5-fold) $_{L}$ANT/rhVDAC1 level of binding compared to the $_{H}$ANT/rhVDAC1 for 75 mM NaCl was observed. Above 100 mM, the $_{L}$ANT/rhVDAC1 interaction declined by 48–58% after one hour of incubation, $_{L}$ANT/rhVDAC1 interaction was not stable with time. This behavior was not observed for $_{H}$ANT interaction towards rhVDAC1. Although low, the interaction of $_{H}$ANT in the presence of high NaCl concentration remained stable over time.

The ATP/ADP binding sites of ANT are oriented either to the inner (matrix, m-state) or to the outer (cytosolic, c-state) face of the IM. Each of these states may be stabilized by binding of a specific high-affinity ligand such as BA for the m-state, and Atra for the

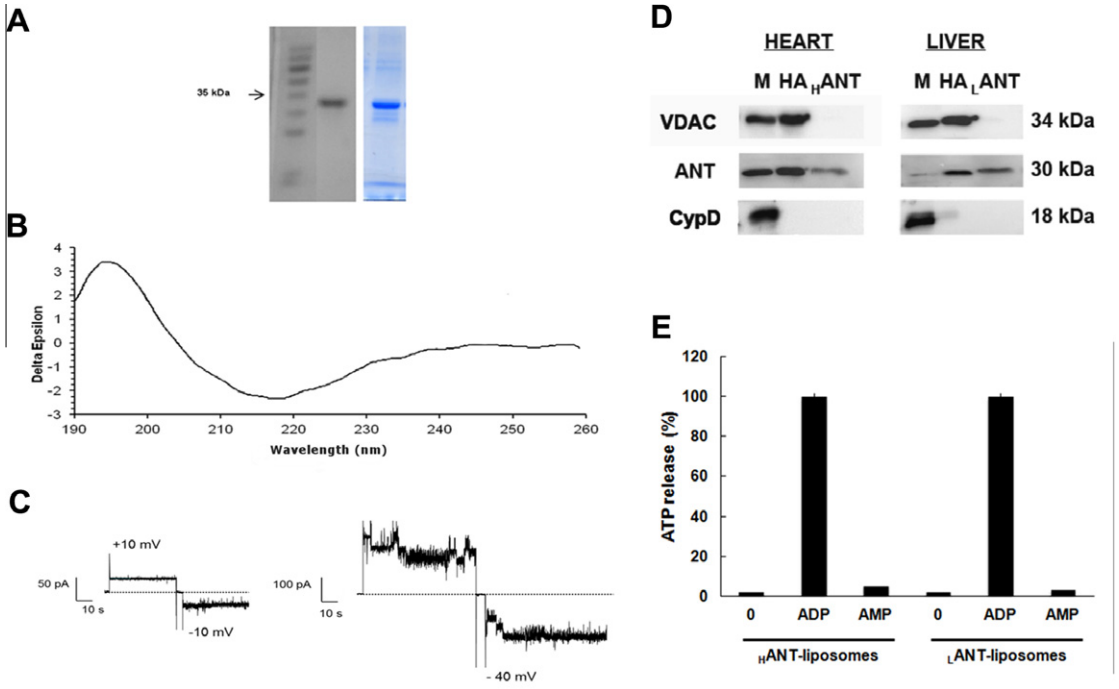

Fig. 2. Proteins production, purification and activity. (A) Western blot and SDS-PAGE of purified rhVDAC1. From left to right: protein ladder, immune revelation by an anti-VDAC polyclonal rabbit serum, Coomassie blue staining. The calculated molecular weight for rhVDAC1 is 32 kDa. (B) Far-UV CD spectrum of refolded rhVDAC1 (0.5 mg/mL) in 25 mM sodium phosphate pH = 7.0, 100 mM NaCl, 1 mM EDTA, 2% LDAO buffer, at 20 °C in a 0.5 mm path length cell. (C) Current traces from VDAC single channels. Upper part, applied voltage was ±10 mV; lower part, applied voltage was ±40 mV; the dashed lined represents the zero current level. (D) $_{H}$ANT was purified from rat heart and $_{L}$ANT from rat liver; their purity was analyzed by western-blotting after SDS–PAGE. The presence of ANT, VDAC and CypD was checked in isolated mitochondria (M), in hydroxyapatite fraction (HA) and in enriched fractions ($_{H}$ANT and $_{L}$ANT). (E) The ADP/ATP exchange activity of ANT was measured into proteoliposomes. The ATP release induced by ADP or AMP addition was evaluated by bioluminescence and expressed as percentage of 400 μM ADP. Experiments were done in triplicate into black 96 well-microtiter plates.

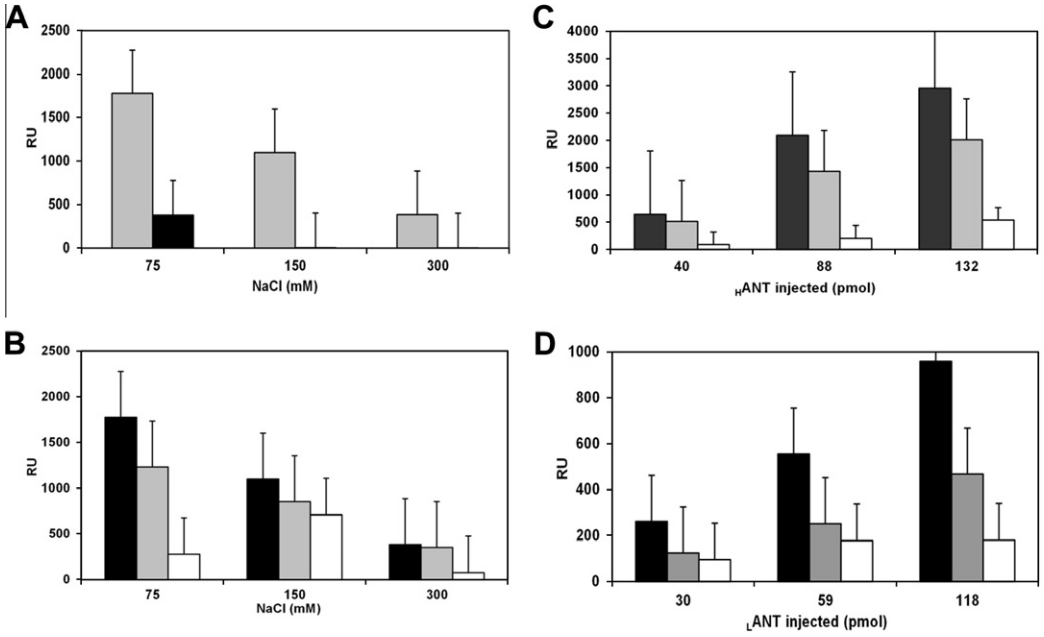

Fig. 3. $_{L}$ANT and $_{H}$ANT isoforms interactions with rhVDAC1. The levels of binding of ANTs to immobilized rhVDAC1 (about 1200 RU) are plotted as histograms in RU (resonance units). The NaCl concentration was set upon ANTs overnight dialysis. The bars represent ±SD for three independent experiments. (A) $_{H}$ANT *versus* $_{L}$ANT interaction. The grey bar represents $_{H}$ANT (injection of 105 pmol), the black bar is for $_{L}$ANT (injection of 47 pmol) (B) $_{H}$ANT interaction as a function of conformation and NaCl concentration. 105 pmol of $_{H}$ANT were injected per assay. Filled black bars represents $_{H}$ANT control interactions, grey bars $_{H}$ANT + BA (50 μM), white bars $_{H}$ANT + Atra (250 μM). Interactions of $_{H}$ANT (C) and $_{L}$ANT (D) with immobilized rhVDAC1 for 75 mM NaCl; filled black bars represents ANT control interactions, grey bars ANTs + BA, white bars ANTs + Atra.

c-state [30–32]. An excess of BA (50 μM) or Atra (250 μM) was added immediately at the end of the purification steps of ANTs. Untreated $_{H}$ANT (Control ANT), $_{H}$ANT + BA and $_{H}$ANT + Atra were injected on top of the rhVDAC1 surface for three salt

concentrations (Fig. 3B). As expected, the level of $_{H}$ANT and $_{L}$ANT bound to immobilized VDAC was dependent of protein concentration and decreased when increasing the salt concentration (Fig. 3B–D). Moreover, in the presence of BA, the binding level of $_{H}$ANT was found to decrease by 30–50% and when $_{H}$ANT was purified in the presence of Atra, its interaction with rhVDAC1 was decreased by 80%. The binding of $_{H}$ANT to VDAC was stable for 5 hours and could be reversed upon injection of 0.5% SDS, a denaturing surfactant. A similar behavior was observed for the interaction of $_{L}$ANT with the rhVDAC1 surface (Fig. 3D). In the presence of BA, the binding level of $_{L}$ANT was found to decrease by 50% and when ANT was purified in the presence of Atra, its interaction with VDAC was decreased by 80%.

4. Discussion

Many evidences support a functional interaction of ANT and VDAC to facilitate metabolites channeling between cytosol and mitochondrial matrix in physiological as well as in pathological models, but structural knowledge of this interaction is scarce. Here, experiments in cardiac and hepatic isolated mitochondria showed clearly that pharmacological manipulation of ANT conformation by Atra and BA affects differentially mitochondrial membrane permeability as shown by swelling and $\Delta\Psi$m measurements. This means that ANT conformation can impact indirectly on the entry of water, solutes and metabolites into mitochondria, which is believed to occur, at least in part, through VDAC channels. In addition, mass spectrometry analysis revealed that all isoforms of VDAC and ANT1 and 2 can be found in immune complex(es). This confirmed the existence of an ANT-VDAC interaction, but did not allow determining whether there is one unique complex or several sub complexes with some preferential ANT/VDAC isoform associations.

Therefore, to gain more insights into the organization and the regulation of the ANT-VDAC interaction, we purified ANT and VDAC from various sources and reconstituted them in a previously described biomimetic system. rhVDAC1 was produced in *E. coli* and was refolded in 2% LDAO buffer. This surfactant was chosen according to the comparative yields obtained for refolding VDAC using different detergents and to mimic the conditions of co-immunoprecipitation. The 15 μM protein fraction was more than 95% pure as shown on SDS-PAGE gel. This protein micellar solution was homogeneous and monodisperse with an hydrodynamic radius of 65 ± 3 nm as attested by quasi elastic light scattering measurements. rhVDAC1 show a similar folded conformation with high β-sheet content similar to previous studies of mitochondrial and refolded VDAC [33,34]. Single channel recordings show a permanently open state at low membrane potentials while closing events and numerous sub conductance states were observed at higher voltages. This is one of the classical hallmarks of VDAC previously described [3,35]. These results demonstrated that a full active rhVDAC1 was produced.

rhVDAC1 was immobilized via its Histag C terminus on top of an Ni NTA surface for SPR binding measurements. 0.4 μM rhVDAC1 injections lead to a surface coverage of 1000–1800 RU (1–2 ng/mm2) of protein. This coverage corresponds to half of a monolayer of immobilized rhVDAC1 and this chip serve as platform to investigate ANTs/rhVDAC1 interactions. NaCl concentration was found to be a crucial parameter for ANT/rhVDAC1 interactions. As NaCl concentration increased, the interaction of $_{H}$ANT and $_{L}$ANT with immobilized rhVDAC1 was lowered. $_{L}$ANT interaction with rhVDAC1 was 4- to 5-folds lower than that measured with $_{H}$ANT and was abolished for NaCl concentrations above 100 mM. This may be explained by a lower $_{L}$ANT/rhVDAC1 affinity than that observed for $_{H}$ANT isoform. Indeed, from experiments performed at 150 mM NaCl with different ANT injected concentrations we estimated a K_D of around 140 nM for $_{H}$ANT, while that of $_{L}$ANT was around 310 nM (Fig. 4). These results are in accordance with results showing that ANT ATP/ADP translocase activity can be blocked for high chloride concentration (above 200 mM) [36]. The authors explained this observation by the shielding of positive charges within the ANT binding site. This was confirmed by combining experimental investigations and molecular-dynamic simulation experiments that revealed a strong modification on the topology of local electric field related to the number of chloride ions inside the ANT cavity [37].

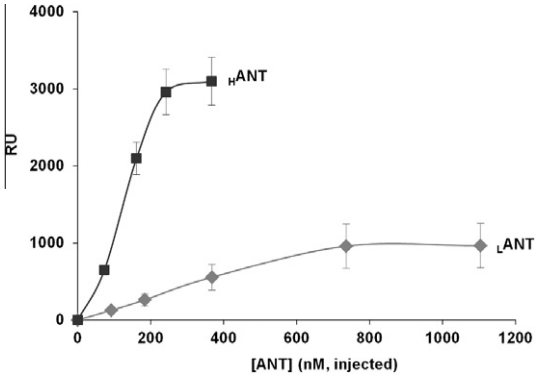

Fig. 4. Determination of $_{H}$ANT and $_{L}$ANT affinity constants for rhVDAC 1 interaction. The binding capacity of ANT for immobilized rhVDAC1 is plotted for different protein concentrations $_{H}$ANT (squares) and $_{L}$ANT (triangles) at 150 mM NaCl. The bars represent ±SD for three independent experiments.

The conformation of ANTs can be blocked by high affinity binding ligands, BA for the m-state, and Atra for the c-state. For $_{H}$ANT control, $_{H}$ANT + BA and $_{H}$ANT + atra, the interaction with the immobilized rhVDAC1 decreased when the salt concentration increased in a similar manner. The level of both ANTs bound to immobilized rhVDAC1 was concentration dependent and their interaction was modulated by the two ligands BA and Atra. rhVDAC1 can interact either with $_{H}$ANT (mainly ANT1) and $_{L}$ANT (mainly ANT2), the affinity of VDAC being better for $_{H}$ANT than for $_{L}$ANT. In the m-state (presence of BA), the binding level was found to decrease by 30–50% for $_{H}$ANT and 50% for $_{L}$ANT. In the c-state (presence of Atra) the level of binding dropped by 80% for both ANT isoforms.

In conclusion, both types of experiments used in this study underscore the effect of ANT conformation and the role of isoform identity on the ANT-VDAC interaction. The SPR platform, which allows the real time measurement of the protein–protein interaction, will be a useful tool for the basic study of putative partners of VDAC or ANT and the development of new therapeutics targeting the ANT-VDAC interaction.

Acknowledgments

The work has been funded by l'Agence Nationale pour la Recherche (ANR-08PCVI-0008-01). CB laboratory is a member of the Laboratory of Excellence LERMIT supported by a grant from ANR (ANR-10-LABX-33). We are grateful to Martine Pugniere (PP2I platform at CRLC) for the access to the Biacore Instrument.

References

[1] G. Kroemer, L. Galluzzi, C. Brenner, Mitochondrial membrane permeabilization in cell death, Physiol. Rev. 87 (2007) 99–163.
[2] A. Messina, S. Reina, F. Guarino, V. De Pinto, VDAC isoforms in mammals, Biochim. Biophys. Acta 12 (2011) 12.
[3] S. Hiller, R.G. Garces, T.J. Malia, V.Y. Orekhov, M. Colombini, G. Wagner, Solution structure of the integral human membrane protein VDAC-1 in detergent micelles, Science 321 (2008) 1206–1210.

[4] V. Shoshan-Barmatz, D. Ben-Hail, VDAC, a multi-functional mitochondrial protein as a pharmacological target, Mitochondrion 12 (2012) 24–34.
[5] F. Palmieri, C.L. Pierri, Mitochondrial metabolite transport, Essays Biochem. 47 (2010) 37–52.
[6] E. Pfaff, M. Klingenberg, Adenine nucleotide translocation of mitochondria. 1. Specificity and control, Eur. J. Biochem. 6 (1968) 66–79.
[7] N. Brustovetsky, M. Klingenberg, Mitochondrial ADP/ATP carrier can be reversibly converted into a large channel by Ca^{2+}, Biochemistry 35 (1996) 8483–8488.
[8] A. Ruck, M. Dolder, T. Wallimann, D. Brdiczka, Reconstituted adenine nucleotide translocase forms a channel for small molecules comparable to the mitochondrial permeability transition pore, FEBS Lett. 426 (1998) 97–101.
[9] C. Brenner, H. Cadiou, H.L. Vieira, N. Zamzami, I. Marzo, Z. Xie, B. Leber, D. Andrews, H. Duclohier, J.C. Reed, G. Kroemer, Bcl-2 and Bax regulate the channel activity of the mitochondrial adenine nucleotide translocator, Oncogene 19 (2000) 329–336.
[10] E. Pebay-Peyroula, C. Dahout-Gonzalez, R. Kahn, V. Trezeguet, G.J. Lauquin, G. Brandolin, Structure of mitochondrial ADP/ATP carrier in complex with carboxyatractyloside, Nature 426 (2003) 39–44.
[11] G. Beutner, A. Ruck, B. Riede, W. Welte, D. Brdiczka, Complexes between kinases, mitochondrial porin and adenylate translocator in rat brain resemble the permeability transition pore, FEBS Lett. 396 (1996) 189–195.
[12] B. Faustin, R. Rossignol, A. Deniaud, C. Rocher, S. Claverol, M. Malgat, C. Brenner, T. Letellier, The respiratory-dependent assembly of ANT1 differentially regulates Bax and Ca^{2+} mediated cytochrome c release, Front Biosci. (Elite Ed.) 3 (2011) 395–409.
[13] C. Chen, Y. Ko, M. Delannoy, S.J. Ludtke, W. Chiu, P.L. Pedersen, Mitochondrial ATP synthasome: three-dimensional structure by electron microscopy of the ATP synthase in complex formation with carriers for Pi and ADP/ATP, J. Biol. Chem. 279 (2004) 31761–31768.
[14] C. Brenner, K. Subramaniam, C. Pertuiset, S. Pervaiz, Adenine nucleotide translocase family: four isoforms for apoptosis modulation in cancer, Oncogene 30 (2011) 883–895.
[15] I. Marzo, C. Brenner, N. Zamzami, S.A. Susin, G. Beutner, D. Brdiczka, R. Remy, Z.H. Xie, J.C. Reed, G. Kroemer, The permeability transition pore complex: a target for apoptosis regulation by caspases and Bcl-2-related proteins, J. Exp. Med. 187 (1998) 1261–1271.
[16] D. Brdiczka, G. Beutner, A. Ruck, M. Dolder, T. Wallimann, The molecular structure of mitochondrial contact sites their role in regulation of energy metabolism and permeability transition, Biofactors 8 (1998) 235–242.
[17] A.S. Belzacq-Casagrande, C. Martel, C. Pertuiset, A. Borgne-Sanchez, E. Jacotot, C. Brenner, Pharmacological screening and enzymatic assays for apoptosis, Front Biosci. 14 (2009) 3550–3562.
[18] J.W. Palmer, B. Tandler, C.L. Hoppel, Biochemical properties of subsarcolemmal and interfibrillar mitochondria isolated from rat cardiac muscle, J. Biol. Chem. 252 (1977) 8731–8739.
[19] Y. Shi, C. Jiang, Q. Chen, H. Tang, One-step on-column affinity refolding purification and functional analysis of recombinant human VDAC1, Biochem. Biophys. Res. Commun. 303 (2003) 475–482.
[20] T.J. Malia, G. Wagner, NMR structural investigation of the mitochondrial outer membrane protein VDAC and its interaction with antiapoptotic Bcl-xL, Biochemistry 46 (2007) 514–525.
[21] A. Deniaud, C. Rossi, A. Berquand, J. Homand, S. Campagna, W. Knoll, C. Brenner, J. Chopineau, Voltage-dependent anion channel transports calcium ions through biomimetic membranes, Langmuir 23 (2007) 3898–3905.
[22] A.S. Belzacq, C. Brenner, The adenine nucleotide translocator: a new potential chemotherapeutic target, Curr. Drug Targ. 4 (2003) 517–524.
[23] C. Martel, M. Allouche, D.D. Esposti, E. Fanelli, C. Boursier, C. Henry, J. Chopineau, G. Calamita, G. Kroemer, A. Lemoine, C. Brenner, GSK3-mediated VDAC phosphorylation controls outer mitochondrial membrane permeability during lipid accumulation, Hepatology 2012 (2012) 25967.
[24] D.R. Hunter, R.A. Haworth, The Ca^{2+}-induced membrane transition in mitochondria. I. The protective mechanisms, Arch. Biochem. Biophys. 195 (1979) 453–459.
[25] P.V. Vignais, P.M. Vignais, G. Defaye, Adenosine diphosphate translocation in mitochondria. Nature of the receptor site for carboxyatractyloside (gummiferin), Biochemistry 12 (1973) 1508–1519.
[26] G.J. Lauquin, P.V. Vignais, Interaction of (3H) bongkrekic acid with the mitochondrial adenine nucleotide translocator, Biochemistry 15 (1976) 2316–2322.
[27] P. Barath, K. Luciakova, Z. Hodny, R. Li, B.D. Nelson, The growth-dependent expression of the adenine nucleotide translocase-2 (ANT2) gene is regulated at the level of transcription and is a marker of cell proliferation, Exp. Cell Res. 248 (1999) 583–588.
[28] J. Lunardi, O. Hurko, W.K. Engel, G. Attardi, The multiple ADP/ATP translocase genes are differentially expressed during human muscle development, J. Biol. Chem. 267 (1992) 15267–15270.
[29] G. Stepien, A. Torroni, A.B. Chung, J.A. Hodge, D.C. Wallace, Differential expression of adenine nucleotide translocator isoforms in mammalian tissues and during muscle cell differentiation, J. Biol. Chem. 267 (1992) 14592–14597.
[30] B.B. Buchanan, W. Eiermann, P. Riccio, H. Aquila, M. Klingenberg, Antibody evidence for different conformational states of ADP, ATP translocator protein isolated from mitochondria, Proc. Natl. Acad. Sci. USA 73 (1976) 2280–2284.
[31] H. Erdelt, M.J. Weidemann, M. Buchholz, M. Klingenberg, Some principle effects of bongkrekic acid on the binding of adenine nucleotides to mitochondrial membranes, Eur. J. Biochem. 30 (1972) 107–122.
[32] B. Scherer, M. Klingenberg, Demonstration of the relationship between the adenine nucleotide carrier and the structural changes of mitochondria as induced by adenosine 5′-diphosphate, Biochemistry 13 (1974) 161–170.
[33] L. Shao, K.W. Kinnally, C.A. Mannella, Circular dichroism studies of the mitochondrial channel VDAC, from Neurospora crassa, Biophys. J. 71 (1996) 778–786.
[34] B. Shanmugavadivu, H.J. Apell, T. Meins, K. Zeth, J.H. Kleinschmidt, Correct folding of the beta-barrel of the human membrane protein VDAC requires a lipid bilayer, J. Mol. Biol. 368 (2007) 66–78.
[35] M. Colombini, Structure and mode of action of a voltage dependent anion-selective channel (VDAC) located in the outer mitochondrial membrane, Ann. NY. Acad. Sci. 341 (1980) 552–563.
[36] T. Gropp, N. Brustovetsky, M. Klingenberg, V. Muller, K. Fendler, E. Bamberg, Kinetics of electrogenic transport by the ADP/ATP carrier, Biophys. J. 77 (1999) 714–726.
[37] E.M. Krammer, S. Ravaud, F. Dehez, A. Frelet-Barrand, E. Pebay-Peyroula, C. Chipot, High-chloride concentrations abolish the binding of adenine nucleotides in the mitochondrial ADP/ATP carrier family, Biophys. J. 97 (2009) L25–L27.